Clim Dyn
DOI 10.1007/s00382-014-2221-6

Impact of the soil hydrology scheme on simulated soil moisture memory

Stefan Hagemann · Tobias Stacke

Received: 15 November 2013 / Accepted: 17 June 2014

Abstract Soil moisture–atmosphere feedback effects play an important role in several regions of the globe. For some of these regions, soil moisture memory may contribute significantly to the state and temporal variation of the regional climate. Identifying those regions can help to improve predictability in seasonal to decadal climate forecasts. In order to accurately simulate soil moisture memory and associated soil moisture–atmosphere interactions, an adequate representation of soil hydrology is required. The present study investigates how different setups of a soil hydrology scheme affect soil moisture memory simulated by the global climate model of the Max Planck Institute for Meteorology, ECHAM6/JSBACH. First, the standard setup is applied in which soil water is represented by a single soil moisture reservoir corresponding to the root zone. Second, a new five layer soil hydrology scheme is introduced where not only the root zone is differentiated into several layers but also layers below are added. Here, three variants of the new scheme are utilized to analyse how different characteristics of the soil hydrology and the associated fluxes influence soil moisture memory. Soil moisture memory of the different setups is analysed from global ECHAM6/JSBACH simulations forced by observed SST. Areas are highlighted where the regional climate seems to be sensitive to the improved representation of soil hydrology in the new setup and its variants. Results indicate that soil moisture memory is generally enlarged in regions during the dry season where a soil moisture buffer is present below the root zone due to the 5-layer scheme. This effect is usually enhanced when this buffer is increased. Memory tends to be weakened (strengthened) where bare soil evaporation is increased (decreased), especially in semi-arid regions and wet seasons. For some areas, this effect is compensated by a decreased (increased) transpiration.

Keywords Soil moisture · Large-scale hydrology · Climate modelling · Soil moisture memory · Land surface processes

1 Introduction

Predictions of the global climate depend on both the model's initial state and the anticipated change in aerosols and greenhouse gases. For decadal predictions anthropogenic climate change and natural variability are expected to be equally important. A close representation of the observed climate state in global coupled climate models is therefore crucial for (the initialization of) decadal predictions. However, predictability beyond 2 weeks is essentially influenced by time scales which are longer than the typical scales of weather phenomena. These slow components which affect seasonal to decadal predictability of the Earth system by their "memory" are not only the oceans, glaciers and sea ice, but also the moisture content of the soil, snow cover and the terrestrial biosphere (Rowntree 1991; Mitchell et al. 2004; Rodell et al. 2004).

Soil moisture controls the partitioning of the available energy into latent and sensible heat fluxes and conditions the amount of surface runoff. By controlling evapotranspiration, it is linking the energy, water and carbon fluxes (Koster et al. 2004a; Dirmeyer et al. 2006; Seneviratne and Stöckli 2008). Thus, soil moisture–atmosphere feedback effects play an important role for the regional climate in

S. Hagemann (✉) · T. Stacke
Max Planck Institute for Meteorology, Bundesstr. 53, 20146 Hamburg, Germany
e-mail: stefan.hagemann@zmaw.de; stefan.hagemann@mpimet.mpg.de

Published online: 26 June 2014

several regions of the globe (e.g. Koster et al. 2004a; Seneviratne et al. 2006b; Taylor and Ellis 2006; Hirschi et al. 2011; see also Seneviratne et al. 2010 for an overview). For some of these regions, soil moisture memory can contribute significantly to such land-climate interactions (e.g. Delworth and Manabe 1988; Koster and Suarez 2001; Seneviratne et al. 2006a) and the development of the regional climate on up to seasonal time-scales (e.g. Schlosser and Milly 2002; Koster et al. 2004b, 2010; Lorenz et al. 2010). Identifying those regions can help to improve predictability in seasonal to yearly climate predictions. In order to ably simulate soil moisture memory and associated soil moisture–atmosphere interactions, an adequate representation of soil hydrology is necessary.

The aim of the present study is twofold. On one hand we introduce a new soil hydrology scheme for the land surface component of the Earth System Model (ESM) of the Max Planck Institute for Meteorology (MPI-M), MPI-ESM. On the other hand we want to shed light on how certain characteristics in a land surface scheme affect the simulated soil moisture memory. Soil moisture memory effects shall be identified by using the atmosphere/land components of MPI-ESM with four different model configurations of the soil hydrology scheme. The first configuration uses the standard setup ("bucket scheme") from the currently operational version of MPI-ESM, in which soil water is represented by a single layer soil moisture reservoir. The second setup uses a new five layer soil hydrology (5-layer) scheme which differentiates the soil column into several layers and expands the soil representation below the root zone. For the 5-layer scheme, two further variants are considered: one where the bare soil evaporation was modified compared to the 5-layer scheme formulation and one where a different dataset of soil water holding capacities was used. The different soil hydrology schemes are described in Sect. 2 with a focus on the newly developed 5-layer scheme. Also the setup of the associated global climate simulations is presented. In Sect. 3, the climate model results using the 5-layer scheme are compared to the standard model results obtained with the bucket scheme and evaluated against observations. The distribution of soil moisture memory and the different impacts of the various soil hydrology characteristics on the simulated memory are considered in Sect. 4. Finally, Sect. 5 ends with a summary and conclusions.

2 Model description and datasets used

2.1 The climate model

For global climate simulations at T63 spatial resolution (ca. 1.875° ≈about 200 km), the atmospheric GCM ECHAM6 (Stevens et al. 2013) with its land surface scheme JSBACH (Raddatz et al. 2007; Brovkin et al. 2009) has been used. ECHAM6 operates with a discrete (0/1) land sea mask.

JSBACH is a state-of-the art ESM land surface scheme that simulates water, energy and carbon related processes including interactive and dynamic vegetation. Its representation of physical processes (with regard to energy and water) at the land surface mostly agrees with those from ECHAM4 (Roeckner et al. 1996). This comprises the separation of rainfall and snow melt into surface runoff and infiltration and the calculation of lateral drainage following the Arno scheme (Dümenil and Todini 1992). Soil moisture W_S is represented by a single-layer ("bucket scheme") whose maximum depth W_{cap} is spatially varying and taken from the LSP2 (Land Surface Parameter version 2) dataset (Hagemann 2002). This maximum water depth corresponds to the root zone, and no water below it is considered. Other vegetation dependent land surface parameters are calculated interactively based on distributions of plant functional types (PFTs) that are taken from the same source dataset as the LSP2 data. In JSBACH a prognostic equation for the amount of snow on the canopy has been introduced, and the calculation of the surface albedo over snow covered areas was modified (Roesch et al. 2001). Contributions to evapotranspiration over land can occur from four fractions of a grid box. Evaporation over snow and from the so-called skin reservoir, i.e. the wet skin fraction of a gridbox that depends on the leaf area index (LAI), occur both at their potential rate. Transpiration from the dry vegetated part of a gridbox is calculated based on Sellers et al. (1986) and depends on the relative soil moisture W_S/W_{cap} and a stomatal resistance, which is a function of the LAI. In the dry non-vegetated part of a grid box, bare soil evaporation E_{bs} is calculated as (Roeckner et al. 1996):

$$E_{bs} = \rho \cdot C_h \cdot |v_h| \cdot (q_v - h \cdot q_{sat}) \tag{1}$$

Here, q_{sat} is the saturation specific humidity at the given surface temperature and pressure, q_v is the specific humidity of the air level direct above surface, v_h is the horizontal wind speed at the surface, C_h is the transfer coefficient for heat, ρ is the density of air. The relative humidity h at the surface is defined as

$$h = \frac{\left(1 - \cos\left(\pi \cdot \frac{W_S - W_{cap} - W_{top}}{W_{top}}\right)\right)}{2} \tag{2}$$

for $W_S > W_{cap} - W_{top}$, $h = 0$ otherwise, with $W_{top} = 0.1$ m for $W_{cap} > 0.1$ m, $W_{top} = W_{cap}$ otherwise. For the calculation of soil temperatures the concept of heat diffusion is used. The heat conduction equation is solved for five layers over land, following Warrilow et al. (1986). Freezing and melting processes within the soil are not taken into account.

2.2 Five layer soil hydrology scheme

In this section, the new five layer soil hydrology scheme is introduced and Fig. 1 is used for illustration to compare the 5-layer scheme with the bucket scheme used in the currently operational version of JSBACH. In the bucket scheme, no soil depth is allocated as the bucket's capacity W_{cap} only represents a water depth corresponding to the root zone water content. The processes of infiltration, transpiration and lateral drainage depend on the bucket soil moisture W_S. As defined in Eq. (2), bare soil evaporation can only occur from the upper 10 cm water column of the bucket.

In the 5-layer scheme, five layers with increasing thickness (0.065, 0.254, 0.913, 2.902, and 5.7 m) are defined with a lower boundary at almost 10 m depth. These layers correspond directly to the structure used for soil temperatures (in the current JSBACH version). However, the number of active layers may be limited by the depth until the bed rock. Thus, the soil water content W_i may be greater than 0 only for those layers i = [1,…,5] with a soil depth z above the bedrock as there is no water available for the land surface scheme within the bedrock. Consequently, lateral drainage (ECHAM4 formulation following Dümenil and Todini 1992) may occur only from those layers above the bedrock. The formulation has been slightly modified as now drainage may only occur if the soil moisture exceeds the permanent wilting point (before the threshold was set to 5 % of W_{cap}) as the suction forces of plants are usually stronger than the forces of gravity (e.g. O'Geen 2012). The permanent wilting point is the soil moisture content below which the plants can not extract water from the soil by transpiration as the suction forces of the soil are larger than the transpiration forces of the plants. The rooting depth z_r, which corresponds to the bucket scheme's maximum depth, determines the depth from where water for transpiration may be extracted by plants. In contrast to the bucket scheme, water may exist below the root zone provided the overall soil depth exceeds the rooting depth. Bare Soil Evaporation is occurring only from the uppermost layer.

The vertical movement of volumetric moisture θ along the soil depth z can be characterized by the one-dimensional Richards (1931) Eq. (3). Here, the local change rate of moisture $\partial\theta/\partial t$ is related to vertical diffusion [first term on the right side of Eq. (3)] and percolation by gravitational drainage of water (second term). Both processes are considered separately in the 5-layer scheme.

$$\frac{\partial\theta}{\partial t} = \frac{\partial}{\partial z}\left(D \cdot \frac{\partial\theta}{\partial z}\right) + \frac{\partial K}{\partial z} + S \tag{3}$$

D denotes the soil water diffusivity, K the soil hydraulic conductivity and S comprises source and sink terms due to infiltration, bare soil evaporation and transpiration. The volumetric soil moisture θ averaged over a depth z is related to the absolute soil water content W by $\theta = W/z$.

For numerical and simplicity reasons, the coupled process of percolation and diffusion is represented in JSBACH as two separate processes. Furthermore, both are realized using different methods because the respective approaches yielded an appropriate model behaviour in JSBACH. For the percolation by gravitational drainage, K is calculated with the van Genuchten (1980) method proposed by Disse (1995).

$$K = K_{sat} \cdot \Theta^{0.5} \cdot \left[1 - (1 - \Theta^{1/m})^m\right]^2 \tag{4}$$

with $\Theta = \frac{\theta - \theta_{pwp}}{\theta_{por} - \theta_{pwp}}$ and $m = \frac{PSI}{PSI+1}$.

Here, K_{sat} is the saturated hydraulic conductivity, PSI is the pore size distribution index θ_{por} is the saturated water content of the soil (porosity) and θ_{pwp} is the residual water content of the soil where in this case the permanent wilting point is taken. For simplicity reasons, we limited the gravitational drainage from each soil layer by the wilting point, as for stronger water tensions occurring at lower soil moisture amounts, percolation and plant extraction are both

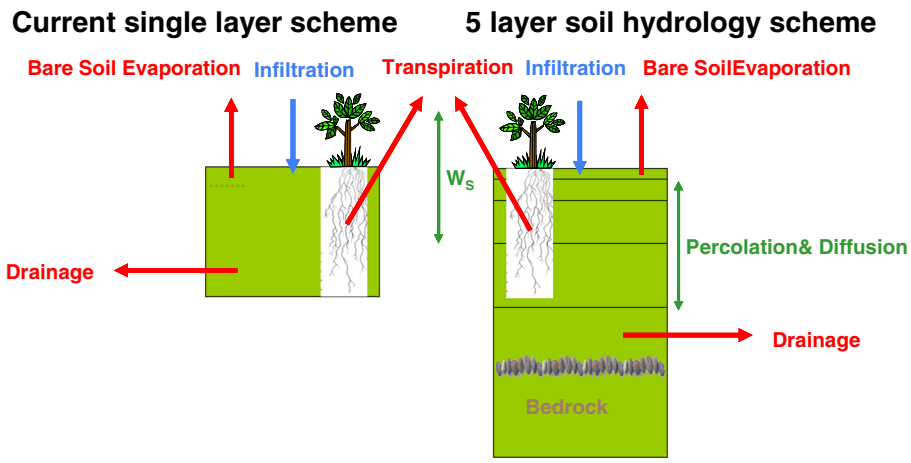

Fig. 1 The single layer bucket (BUCKET) and the 5-layer scheme (5-LAYER, 5L-LSP2, 5L-EXP). See Sect. 2.5 for the definition of the experiment names given in brackets

negligible. In order to discretize the differential expression for percolation, the midpoint method is used. Moreover, to overcome numerical instabilities occurring for large relative soil moisture values Θ, for large time steps and small distances, a maximum percolation flux is set. Note, that there is no percolation of water to the bedrock or below. Even though a specific deep groundwater component like aquifers below the bedrock is not considered, such flow is conceptually simplified and included in the lateral drainage (see above), which seems to be a reasonable assumption on the large ESM grid scales for many areas.

The soil water diffusivity D of each layer is parameterized according to Eq. (5) following Clapp and Hornberger (1978), whereas the diffusivity between two layers is calculated as the average of both layer diffusivities. The soil water diffusion between the layers is treated using the Richtmyer and Morton (1967) diffusion scheme.

$$D = b_{Clapp} \cdot K_{sat} \cdot \frac{\psi_{sat}}{\theta} \cdot \left(\frac{\theta}{\theta_{por}}\right)^{b_{Clapp}+3} \tag{5}$$

Here, Ψ_{sat} is the saturated moisture potential and b_{clapp} is the so-called Clapp & Hornberger parameter. The soil parameter values for the different soil textures based on an improved FAO soil type dataset (K. Dunne, pers. Comm., 2005) are taken from various sources and are summarized in Table 1.

Related to the layered structure for the soil hydrology, there are two major differences between the bucket scheme and the 5-layer scheme. In the bucket scheme, transpiration may occur from the whole soil moisture in the bucket that is above the wilting point over vegetated areas. In the 5-layer scheme, soil water may reside below the root zone, which cannot directly be accessed by plants, but only be transported upwards into the root zone by diffusion following the Richards (1931) equation. Thus, the water below the root zone, which is not present in the bucket scheme, can act as buffer in the transition between wet and dry periods. A second notable difference between the two schemes is related to the formulation of bare soil evaporation. In the bucket scheme, this may only occur if the whole soil moisture bucket is almost completely saturated, while in the 5-layer scheme, it depends only on the saturation state of the uppermost soil layer. This means that Eq. (2) is replaced by Eq. (6):

$$h = \frac{\left(1 - \cos\left(\pi \cdot \frac{W_{S1}}{W_{cap1}}\right)\right)}{2} \tag{6}$$

where W_{S1} and W_{cap1} are the soil moisture and water holding capacity of the uppermost layer, respectively. Here, this upper layer is much thinner than the root zone (bucket) so that bare soil evaporation can occur more frequently, especially after rainfall events.

In addition, representation of bare soil evaporation was modified. During the present study it turned out that the

Table 1 Soil parameter values for the different soil textures

No.	Texture	θ_{por}	θ_{FC}	θ_{pwp}	Ψ_{sat}	Ψ_{sat}	b_{Clapp}	*PSI*
1	Sand	37.31	9.30	3.30	0.0473	23.56	3.3900	0.5920
2	Loamy sand	38.57	17.20	5.80	0.0639	16.56	3.8600	0.4740
3	Sandy loam	41.59	22.90	10.00	0.1319	7.11	4.5000	0.3220
4	Loam	43.48	28.80	14.50	0.2073	4.19	5.7700	0.2200
5	Silt loam	46.76	34.10	15.30	0.4543	1.68	4.9800	0.2110
6	Sandy clay loam	41.59	28.00	15.70	0.1319	7.11	7.2000	0.2500
7	Silty clay loam	47.64	34.50	20.10	0.5610	1.31	8.3200	0.1510
8	Clay loam	44.87	31.70	18.70	0.2889	2.85	8.3200	0.1940
9	Sandy clay	42.35	31.10	18.80	0.1581	5.76	9.5900	0.1680
10	Silty clay	48.14	33.80	20.70	0.6330	1.14	10.3800	0.1270
11	Clay	46.13	38.40	25.00	0.3907	2.00	12.1300	0.1310
12	Coarse	39.77	19.40	8.70	0.0937	13.59	4.7375	0.4095
13	Medium	45.69	32.30	17.20	0.3779	2.51	6.8475	0.1940
14	Fine	45.54	34.40	21.50	0.3939	2.97	10.7000	0.1420
15	Peat	88.00	88.00	25.50	0.0102	2.00	4.0000	0.7000

Volumetric soil porosity θ_{Por} (%), saturated moisture potential Ψ_{sat} (m), saturated hydraulic conductivity Ψ_{sat} (μm/s) and the Clapp and Hornberger (1978) exponent b are taken from Beringer et al. (2001), volumetric soil field capacity θ_{FC} (%) and wilting point θ_{pwp} (%) follow Patterson (1990) and the soil pore size distribution index *PSI* is obtained from Williams and Ahuja (2003). All corresponding values for peat soils are taken from Letts et al. (2000) except for b (Beringer et al. 2001) and θ_{pwp} (Patterson 1990)

initial introduction of the 5-layer scheme led to an unrealistic partitioning of bare soil evaporation and transpiration within several regions. It appeared that the first component was too large which led to a reduction in the latter flux due to soil water depletion (see also Sect. 3.1). This effect could be related to the fact that both water fluxes are accessing the same soil moisture storage. Thus, a separate bare soil moisture storage was introduced for the upper layer of the soil so that bare soil evaporation depends on, and changes only, this storage. Since in reality, bare soil parts and vegetated parts are usually not completely decoupled, we introduced a simplified formulation of lateral diffusion. The diffusivities of the bare soil and the vegetated part of a gridbox, D_{bs} and D_{veg}, are calculated according to Eq. (5). For simplicity it is assumed that lateral diffusion only takes place in 1 % of the gridbox area, so that the mean lateral diffusivity D_l used in the Richtmyer and Morton (1967) diffusion scheme is defined as

$$D_l = \left(\frac{D_{bs} + D_{veg}}{2}\right) \times 0.01 \tag{7}$$

The 5-layer scheme also utilizes a new dataset of soil water holding capacities W_{cap}. These new data were derived from a optimized plant available water (W_{ava}) dataset (Kleidon 2004) by assigning the gridded W_{ava} values to plant types using a multiple linear regression. From plant specific W_{ava} and a land cover specific relative wilting point f_{pwp} (Hagemann 2002), W_{cap} was computed as:

$$W_{cap} = \frac{W_{ava}}{(1 - f_{pwp})} \tag{8}$$

and remapped according to the vegetation cover distribution used in the land surface model. The difference between the new and the operational W_{cap} taken from the LSP2 dataset (Hagemann 2002) is shown in Fig. 2. Major changes are generally related to decreased capacities in arid and semi-arid areas and increased capacities in areas with tropical rain forest.

2.3 Derivation of rooting depth

The rooting depth z_r determines the depth until which transpiration may occur. As the bucket scheme does not include any actual soil depth information, it needed to be derived consistently to the bucket storage capacity W_{cap} to allow comparisons of the 5-layer scheme to the bucket scheme. Thus, z_r was scaled such that the amount of water which is available for transpiration is similar in both schemes. Its computation uses the total soil water holding capacities W_{cap}, either from the LSP2 dataset (Hagemann 2002) used in the bucket scheme or from the new data used in the 5-layer scheme (see above), and the volumetric field capacities θ_{FC} based on a FAO (Food and Agriculture Organization of the United Nations) soil type distribution (FAO/UNESCO 1971–1981) adjusted by Dunne (2005, pers. comm.), which is available at 0.5° resolution. Prior to the computation of the rooting depth z_r distribution W_{cap} data can be aggregated on the

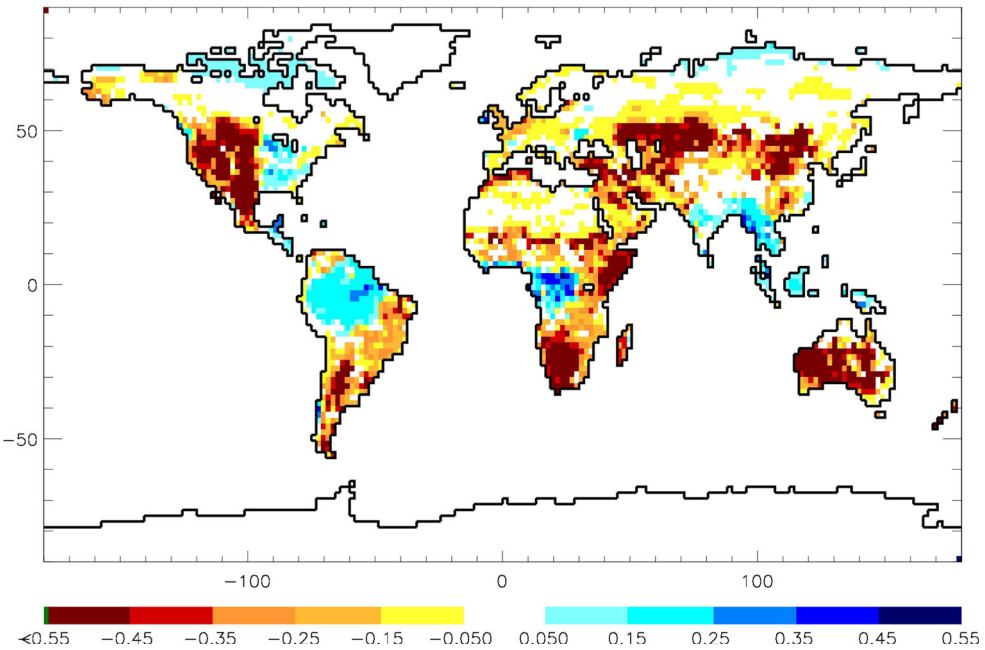

Fig. 2 Difference between the new soil water holding capacities and the operational LSP2 capacities (Hagemann 2002) at T63 resolution. Unit: [m]

desired target resolution while θ_{FC} needs to be interpolated to the respective resolution. z_r is then derived from Eq. (9).

$$z_r = \frac{W_{cap}}{\theta_{FC}} \tag{9}$$

In addition, z_r is limited by the soil depth z_s at which the

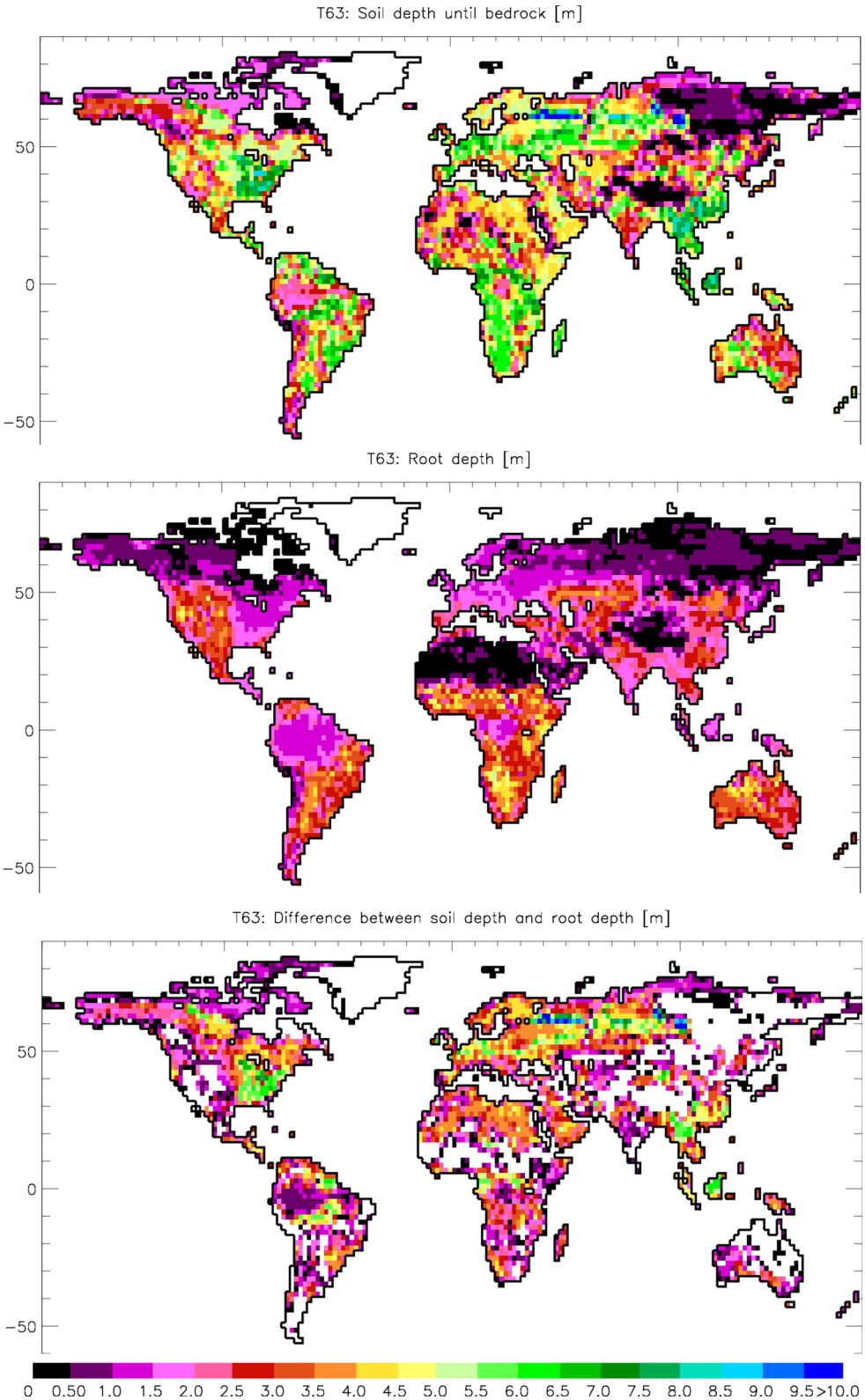

Fig. 3 Soil depth (*upper panel*), root depth (*middle panel*) using LSP2 W_{cap} data and difference between soil depth and root depth (*lower panel*) at T63 resolution. Unit: [m]

bedrock occurs that is derived from the soil type dataset and FAO soil profile data (Dunne and Wilmott 1996):

$$z_r = Min(z_r, z_S) \tag{10}$$

In order to perform this limitation, z_s is also interpolated from the original 0.5° grid to the target resolution. Note that at gridboxes where the rooting depth z_r is shortened due to soil depth limitations, the corresponding W_{cap} is reduced in a consistent way, too. In order to account for grid boxes where the fraction of land is not zero, but no soil type is allocated by Dunne (2005, pers. comm.) the soil depth is set to the rooting depth z_r. The global distributions of z_r and z_s based on the LSP2 dataset are shown in Fig. 3 at T63 resolution (about 1.875° ≈200 km). The difference between z_s and z_r illustrates the added soil water storage below the root zone that is introduced in the 5-layer scheme compared to the bucket scheme.

Note that at gridboxes where the rooting depth z_r and, consequently, W_{cap} are reduced due to limitations in soil depth, the changed W_{cap} is also used in the bucket scheme to be consistent, which may lead to deviations in the results compared to previous simulations with this operational setup.

2.4 Calculation order

The bucket scheme uses the field capacity W_{cap} as the maximum soil water content, and not the saturated water holding capacity as it would be expected from the process scale. This has been done in order to take into account the grid scale of the associated land surface process parameterizations, i.e. that the soil within a coarse GCM gridbox of about 200 × 200 km^2 or coarser is not homogenous, and has cracks and gaps that allow faster flow than within the textured soil itself. A similar approach has been used in the 5-layer scheme. With regard to the calculation of percolation, the volumetric porosity in the original van Genuchten method was replaced by the volumetric field capacity (cf. Eq. 9).

From this point onwards, W_S and W_{cap} only refer to the soil moisture and field capacity until the rooting depth (as it was before), but still the 5-layer scheme takes into account the water content below. While evaporation and/or surface runoff are calculated using root zone W_S and W_{cap}, the resulting soil moisture changes also affect the layers below due to the change in the water content gradient between the layers. After percolation and drainage are calculated, W_S must be updated by the water content within the root zone.

First, moisture changes induced by upward fluxes of transpiration and bare soil evaporation are subtracted from the soil layer water contents W_i, then infiltration is added and the vertical water transport takes place. Technically, half of the infiltration is applied before the computation of the vertical soil water fluxes of percolation and diffusion and the other half afterwards. This is necessary to account for the simultaneously occurring changes of soil moisture in a given layer due to infiltration as well as vertical water transport. Within the soil, gravitational drainage (percolation) amounts are calculated for each layer before the diffusion of water between the layers is conducted. Except for the lowest layer above the bedrock in which no downward percolation is possible, lateral drainage is extracted from the soil moisture layers before diffusion occurs. After the diffusion has changed the soil moisture contents of the layers, the percolation fluxes are used to change the soil moisture contents. Then, the second half of infiltration is added to the soil water, and the root zone soil moisture W_S is updated according to Eq. (11).

$$W_S = \int_0^{z_r} W_{S_i} dz \tag{11}$$

2.5 Simulation setup

The GCM ECHAM6/JSBACH was used to conduct simulations at T63 with 47 vertical layers in the atmosphere. It was forced by observed sea surface temperature (SST) and sea ice from the AMIP2 (Atmospheric Model Intercomparison Project 2) dataset for 1979–1999 (Taylor et al. 2000). In order to identify soil moisture memory effects over different regions and to analyse the impact of the representation of soil hydrology on these effects, a set of four simulations has been conducted:

1. BUCKET using the bucket scheme.
2. 5-LAYER using the 5-layer scheme as described in Sect. 2.2.
3. 5L-LSP2 using a variant of the 5-layer scheme where the soil water holding capacities W_{cap} are taken from the LSP2 dataset (Hagemann 2002) to allow the separation of changes introduced by the changed W_{cap} data from those introduced by the 5-layer scheme structure.
4. 5L-EXP is a sensitivity simulation with the same setup as 5L-LSP2, but using a formulation of bare soil evaporation without the separate bare soil moisture storage for the upper layer of the soil (see Sect. 2.2).

Note that all 5-layer scheme simulations (5L) were preceded by a long-term spin-up (1958–1978) before the actual simulations were started while for the bucket scheme one year spin-up (1978) was sufficient.

3 Evaluation

In this section, the climate model results using the new 5-layer scheme are compared to the bucket scheme results

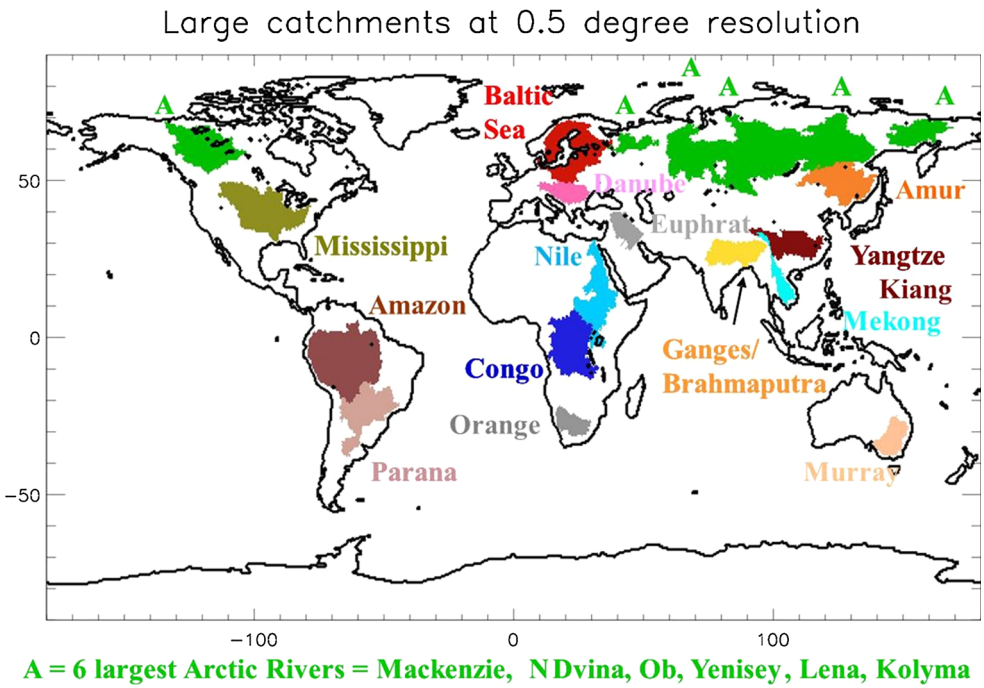

Fig. 4 Location of selected large catchments

and evaluated against observations. As observations, we use the WATCH forcing data (WFD; Weedon et al. 2011) for precipitation (P) and temperature (T), and climatological observed river discharges (Dümenil Gates et al. 2000) for runoff (R). Since the accuracy of global observational evapotranspiration (ET) datasets (e.g. Jiménez et al. 2011; Mueller et al. 2011) is highly uncertain, ET has been diagnosed as $ET = P–R$ by assuming that the long-term storage changes of soil water and snow are negligible. Generally the simulated mean climate is largely similar using the 5-layer scheme compared to the BUCKET simulation (see also below), so that the analysis is focused on selected major catchments of the Earth. For a spatial representation of the general biases in P and T of ECHAM6/JSBACH, see MPI-ESMa in Hagemann et al. (2013). The distribution of catchments selected for the model evaluation is shown in Fig. 4. In order to represent closed hydrological units over the different continents, the largest rivers on Earth are included as well as a few smaller ones in Europe (Baltic Sea, Danube) and Australia (Murray). For the calculation of catchment averages, we used conservative remapping from the T63 grid (see Sect. 2.1) to 0.5° resolution, and then calculated weighted area averages over catchments areas using a 0.5° dataset of catchment masks (see Hagemann and Dümenil 1998).

3.1 Main changes in process representation

The 5-layer scheme leads to an improved representation of soil hydrology processes. On the one hand, there is now water available for bare soil evaporation after a rain event has sufficiently moistened the thin top soil layer. In the bucket scheme, bare soil evaporation is only possible when the whole soil column is sufficiently wet so that water has to be available in the upper 10 cm water column of the bucket (cf. Sect. 2.2). Therefore, almost no bare soil evaporation occurred in medium dry to arid catchments such as for the Orange throughout the whole year or for the Danube in the second half of the year (Fig. 5). With the 5-layer scheme, bare soil evaporation can occur after rain events even if the deeper parts of the soil column are dominated by dry conditions, which is a more realistic behaviour. Figure 5 also shows that the 5-layer scheme would produce a much too strong enhancement of bare soil evaporation in the case that a separate treatment of top layer soil moisture in the bare soil part of a gridbox is not considered (5L-EXP). For the Danube, this leads to unrealistically high values during summer that are even exceeding the transpiration.

On the other hand, the buffering effect of water storage below the root zone is now taken into account. This effect is neglected in the bucket scheme where the transpiration of plants could principally access the water within the whole bucket. The main effect of the water storage below the root zone is that when the root zone soil is depleted by evaporation in the dry season, it can partly be refilled by an upward water transport from below. This leads to an extended water supply for transpiration during the dry season and results in latent heat fluxes that can be sustained longer before they are limited by the drying of the whole

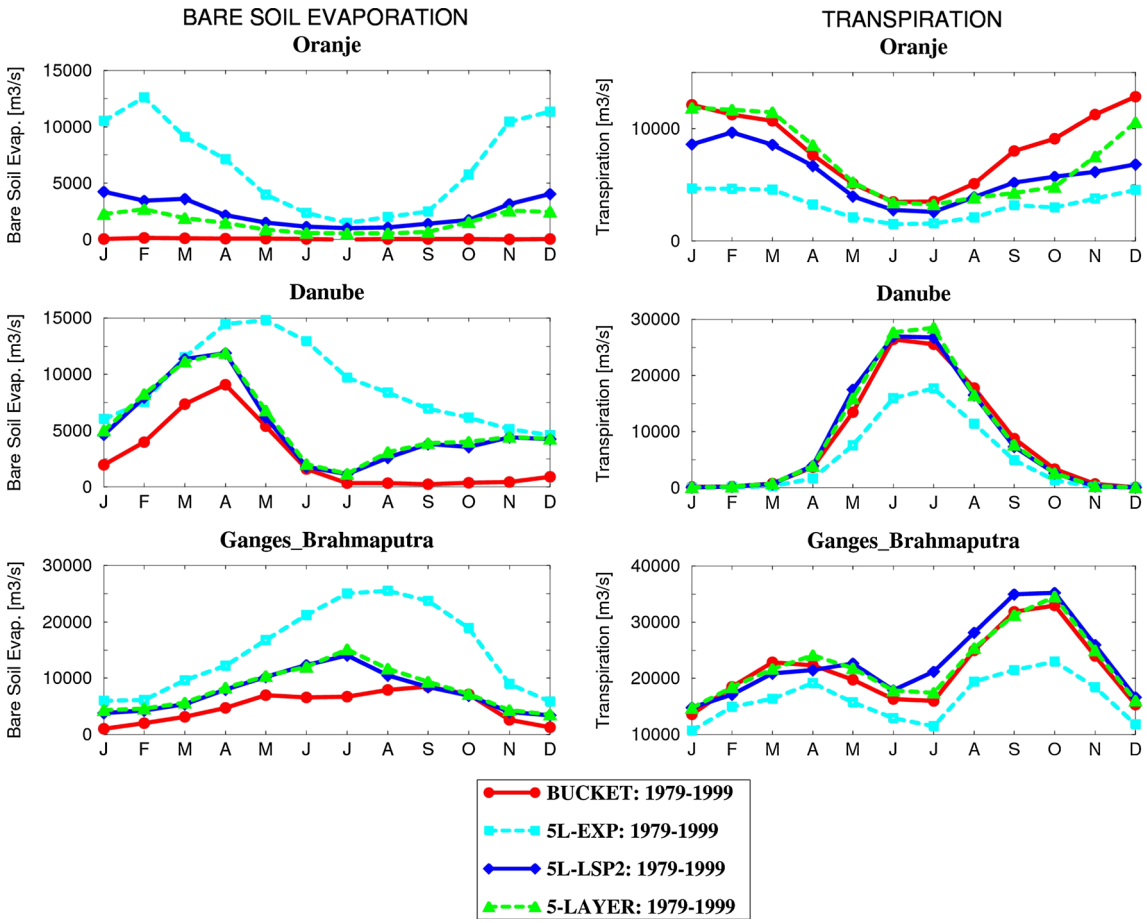

Fig. 5 Catchment averaged bare soil evaporation (*left panel*) and transpiration (*right panel*) over selected catchments

soil column. In this respect, the model representation of soil hydrology becomes more realistic, as it has been shown that there is significant "hydraulic redistribution" by a wide range of plant species across many different biomes around the globe, from deserts to tropical rainforests, which bring water from deep reservoirs to the near-surface soil during dry periods (Caldwell et al. 1998; Jackson et al. 2000).

The consequence for many catchments, such as, e.g. Baltic Sea and Parana, shown in Fig. 6, is that on the one hand the root zone becomes drier in the wet seasons, partially due to an increased bare soil evaporation and partially due to the downward transport of water from the root zone to the buffer below. On the other hand the root zone often becomes wetter in the dry season due to the water supply from the layer below the root zone via an upward transport.

For some of the catchments, mostly located in semi-arid areas, the increase in bare soil evaporation is very prominent, leading to a drier root zone throughout the year (e.g. Danube, Euphrates, Murray, Orange). However, even in those basins the soil moisture decrease is reduced during the dry season due to the buffering effect of water storage below the root zone. For the Nile, the root zone becomes wetter throughout the year. Here, a potential drying in the wetter part of the year (July–October) seems to be overly compensated by an increase in rainfall from July to September in the 5-layer simulation (not shown). For catchments where the dry season occurs during winter when most precipitation falls as snow and hardly any evapotranspiration draws water from the soil, no effects on soil moisture are seen during this period. During the wet season the soil can get drier due to the increased bare soil evaporation (Mississippi) or due to an increased downward transport out of the root zone (Arctic Rivers). A subsequent result of the latter effect is that the snow melt induced surface runoff peak in spring is lower while there is generally a drainage increase throughout the year that is mainly caused by more continuous supply from the soil moisture buffer below the root zone (not shown).

3.2 Comparison to observations

Large-scale annual surface water fluxes do not show pronounced improvements or deteriorations using the

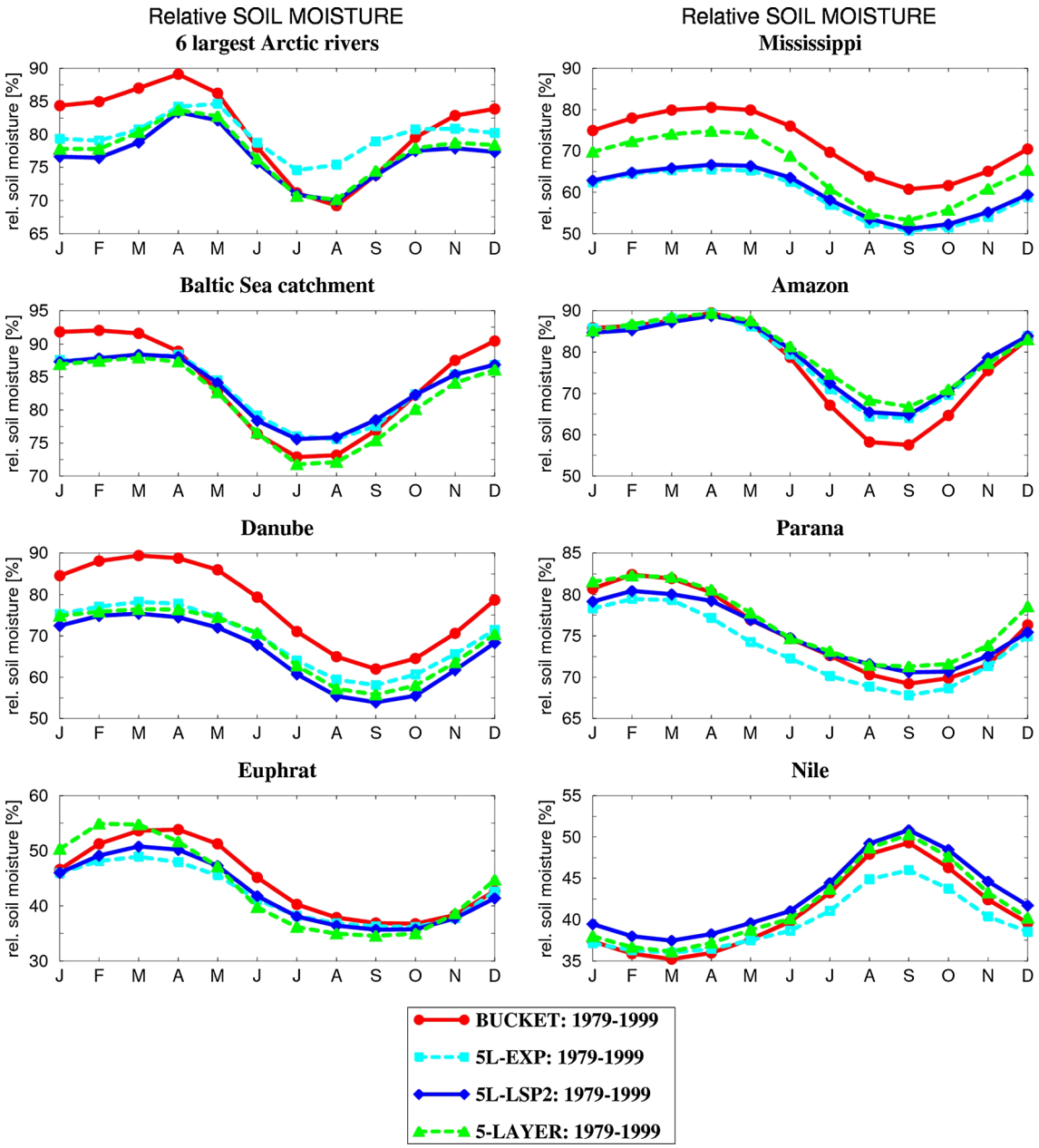

Fig. 6 Relative root zone soil moisture W_S/W_{cap} over selected catchments

5-layerscheme. Thus, the general bias pattern of simulated precipitation agree with those shown for MPI-ESM AMIP simulations by Hagemann et al. (2013; Fig. 4 therein). In order to avoid the direct impact of precipitation biases in the evaluation of hydrological fluxes, we considered evaporation ratio and the runoff coefficient for various catchments instead of the absolute values of evapotranspiration and runoff in Fig. 7. Here, it is shown that increased and decreased biases vary unsystematically between regions and variables. The same applies to the simulated annual mean 2 m temperatures (Fig. 8). As improvements of the large-scale biases in the hydrological cycle are only minor, the main reason for these biases is likely not the representation of soil hydrology.

In order to evaluate the large-scale effect of changes in ET characteristics (i.e. bare soil evaporation and transpiration, cf. Sect. 3.1), we consider the near surface relative air humidity Q_{rel} at 1,000 hPa in Fig. 9. Over several regions, the increases in ET using the 5-layer scheme (5-LAYER and 5L-LSP2) lead to a wide removal (Southern Europe, North America, Australia) or reduction (Middle East, Caucasus, South Asia, Amazonia, Southern

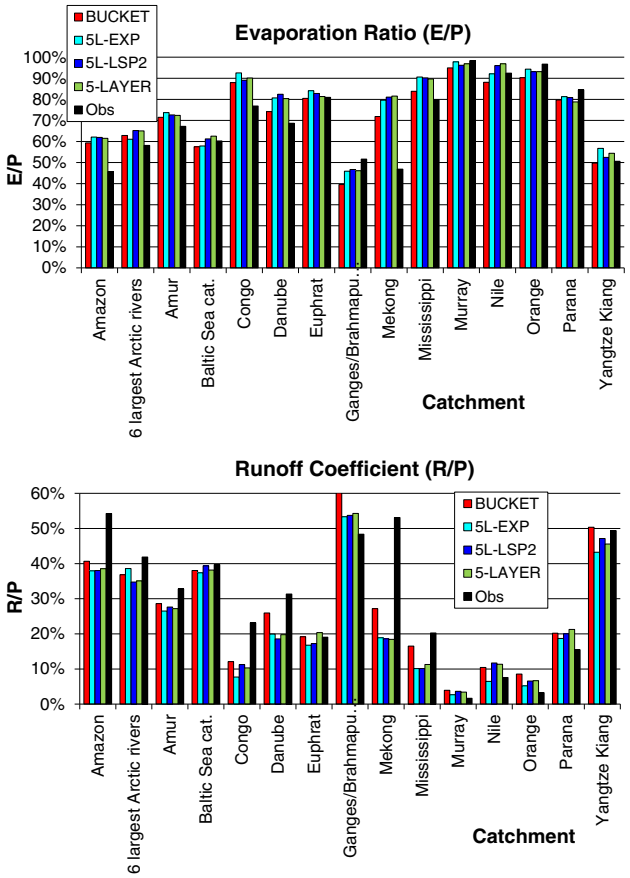

Fig. 7 Evaporation ratio (E/P; *upper panel*) and runoff coefficient (R/P; *lower panel*) over selected large catchments of the globe

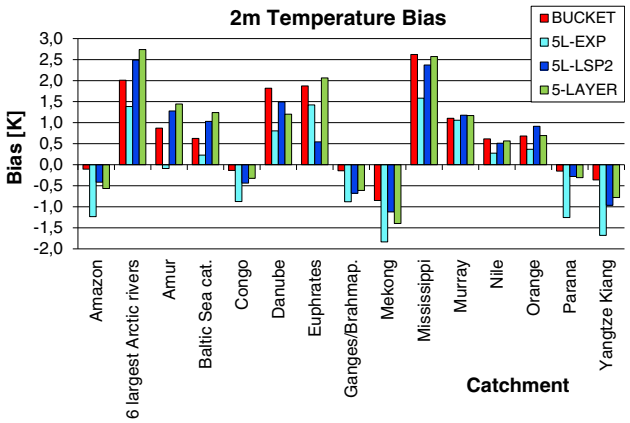

Fig. 8 Annual mean 2 m temperature differences to WFD data over selected large catchments of the globe

Parana, Central Africa) of dry biases in Q_{rel} if compared to ERA-Interim reanalysis data (Dee et al. 2011). The remaining dry biases are likely associated with deficiencies in the atmospheric part (ECHAM6) and the simulation of clouds whose amounts tend to be underestimated in several regions such as indicated by overestimated surface solar incoming radiation (SSI) over Middle East, Caucasus, United States and the Congo region (not shown) if compared to Clouds Earth Radiation Energy System (CERES) data (version CERES EBAF-Surface_Ed2.6r; Kato et al. 2013). Note that on the one hand, dry biases in near-surface humidity may exacerbate positive biases in bare soil evaporation. On the other hand, the overly strong simulation of wet biases in 5L-EXP (Fig. 9b) over Northern Eurasia, eastern and western North America and southern South America suggests that the very strong enhancement of bare soil evaporation is unrealistic in 5L-EXP as these biases are absent or much weaker in 5-LAYER and 5L-LSP2 (Fig. 9c, d).

Associated with ET increases and a wetting of Q_{rel} is a general reduction of the 2 m temperature. If annual mean 2 m temperatures are compared to WFD data, bias differences between the BUCKET and the 5-LAYER simulation are largely blurred by the existing biases, specifically those occurring in boreal winter over mid- and high latitudes of North America and Eurasia as well as Australia (cf. Hagemann et al. 2013). Here, only the 5L-EXP simulation shows a widespread reduction in annual warm biases around the globe (not shown). This might look well for the wrong reason (see also below). If only the boreal summer is considered (Fig. 10), 5-LAYER (Fig. 10d) shows increased warm biases over North America and northern Eurasia compared to BUCKET (Fig. 10a), and reduced warm biases over Southern Europe, India, Amazonia and Central Africa, but these changes are usually weak. For 5L-EXP (Fig. 10b), large cold biases evolve over Northern Eurasia, Western North America and the Sahel. As these contribute to the general cooling in the annual mean, they partially compensate warm biases in other seasons, especially in the boreal winter over the northern mid- and high latitudes (see Amur, Arctic rivers, Baltic Sea, Mississippi in Fig. 8).

However, on the seasonal time scale, several catchments can be identified where improvements in the simulated 2 m temperature can be directly associated with the more realistic behavior of the 5-layer scheme. For the Danube catchment (Fig. 11) the reduced warm bias in the second half of the year can be directly attributed to the increased bare soil evaporation in the 5-layer (5-LAYER, 5L-LSP2). In contrast, the bare soil evaporation is close to Zero using the bucket scheme (BUCKET) during this part of the year. The same seems to apply for the Ganges/Brahmaputra catchment from May to July (JJA; Fig. 11). For the Amazon (Fig. 11), the removal of the warm bias during the dry season (August–October) can be attributed to the moisture supply from the buffer below the root zone. This leads to a wetter root zone during the dry season allowing for higher evapotranspiration rates and the associated latent cooling. For all three catchments, SSI is overestimated (Fig. 12) with the bucket scheme (BUCKET) during the

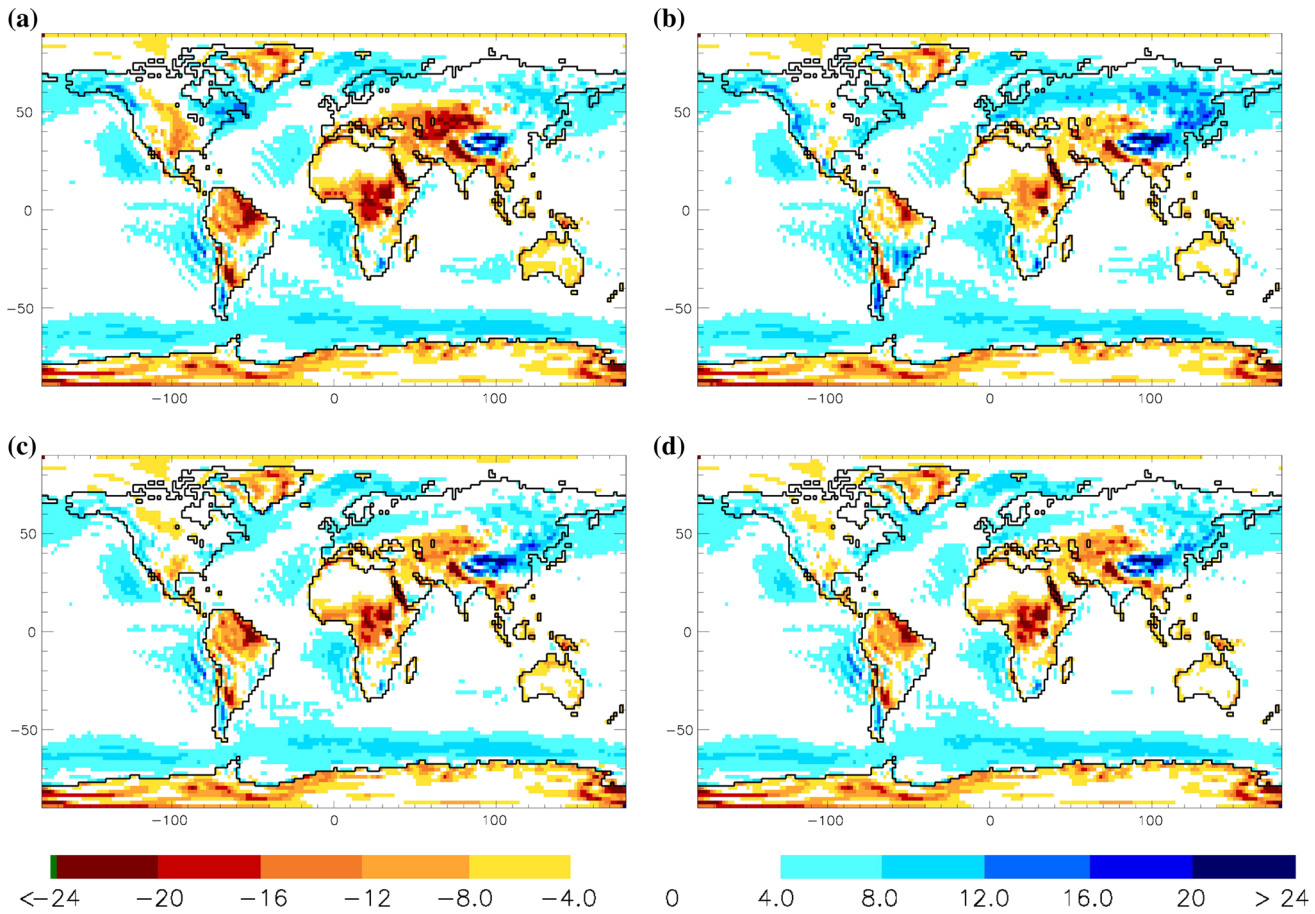

Fig. 9 Annual mean relative air humidity differences (%) at 1,000 hPa to ERA-Interim data for **a** BUCKET, **b** 5L-EXP, **c** 5L-LSP2, and **d** 5-LAYER

time when the warm biases occur (Fig. 11), pointing towards too little cloud cover in the atmosphere. In all 5-layer simulations, SSI is reduced especially when the warm biases are also reduced. This indicates that the increased ET due to the increased bare soil evaporation leads to more upwards transport of moisture, which favours the development of more cloud cover (not shown) so that SSI is reduced, which tends to become closer to the observations, at least in those months where the warm bias and SSI bias were largest using the bucket scheme.

Additional information about the performance of the 5-layer scheme can be found in Loew et al. (2013) who considered an 'offline' JSBACH simulation using the 5L-LSP2 model setup where JSBACH was forced by observational data. They compared the simulated top layer soil moisture to satellite surface moisture measurements from the new ECV_SM dataset (Liu et al. 2011) and found a generally good agreement between both. As these datasets are rather independent from each other, this gives some confidence in the validity of the JSBACH version using the 5-layer scheme.

4 Soil moisture memory

Following Koster and Suarez (2001) and Seneviratne et al. (2006a), soil moisture memory is indicated in regions where anomalies of soil moisture have a persistent autocorrelation. By removing the long-term mean seasonal cycle from the monthly mean soil moisture, we calculated anomaly time series of 252 months for each simulation from which the respective autocorrelation of the total column soil moisture WS_{ges} was derived. In order to highlight longer term memory effects, we considered areas, where the autocorrelation is continuously larger than 0.3 for time lags of several months (see Fig. 13), to be affected by soil moisture memory processes. For all simulations, soil moisture memory effects of one season or longer (3 months or more with autocorrelation >0.3, Figs. 13, 14) can be seen over US, southern South America (Parana) and Africa (Orange), Sahel, South and Central Europe (Danube), Australia, Caucasus and West Siberia, Southern China and Indochina (Mekong). It has to be noted that memory diagnostics may be blurred in essentially dry

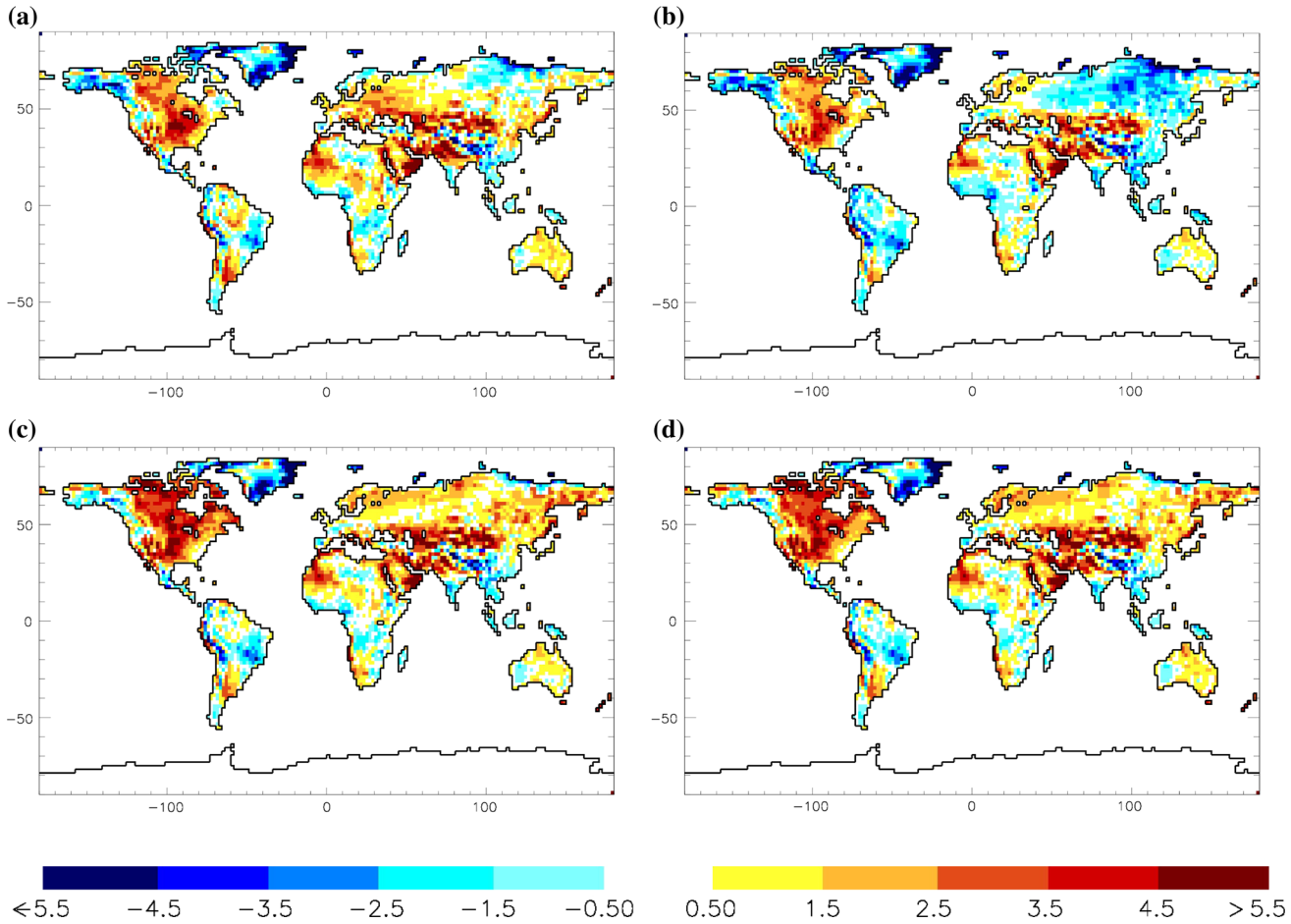

Fig. 10 Summer mean 2 m temperature differences to WFD data for **a** BUCKET, **b** 5L-EXP, **c** 5L-LSP2, and **d** 5-LAYER

regions (e.g. Sahara, Asian deserts, Australia) or areas where the soil is simulated to be almost continuously wet (Northern Siberia). In order to understand the effects of different representations of soil hydrology on the simulated soil moisture memory, these representations are discussed separately in the following.

The most important step in changing the representation of soil hydrology is the replacement of the bucket scheme with a 5-layer scheme. First, we consider the effects of changing the scheme structure by comparing the 5L-LSP2 version to the BUCKET scheme. The 5-layer scheme, due the water buffer below the root zone (cf. Fig. 3), increases soil moisture memory over large parts of the globe (Fig. 15a—left panel, Fig. 14), especially over northern and eastern US (e.g. Mississippi), northern and middle South America (Amazon, Parana), Europe, South East Asia (Mekong) and Central Africa (Congo). It decreases memory, mainly due to enhanced bare soil evaporation (Fig. 15a—right panel) in less vegetated areas, over Eastern US, southern South America, Sahel and South Africa, Australia (Murray) and Northern Siberia. In some areas, both effects on the memory seem to partially compensate each other, even though the increasing impact of the water buffer below the root zone often tends to be stronger. This is, e.g., the case for the Orange catchment where despite the increase in bare soil evaporation, the memory behaviour, i.e. autocorrelation of WS_{ges} as a function of the monthly lag, hardly changes.

As mentioned in Sect. 2.2, the initial implementation of the 5-layer scheme used in 5L-EXP yields generally too large bare soil evaporation. When reducing this in 5L-LSP2 (Fig. 15b—right panel), the associated changes in soil moisture memory are quite patchy (Fig. 15b—left panel). Even though there are areas where memory is somewhat increasing, such as for the Mississippi catchment (Fig. 14), it is decreasing in other areas (e.g. Parana, Congo). This is related to the fact that generally the near surface atmospheric demand for moisture largely determines the total evapotranspiration *ET*, independently whether ET is limited by radiation or soil moisture. Thus, if one of the *ET* components is reduced, this is potentially compensated by moisture fluxes from the other components due to the atmospheric demand. As skin reservoir and snow evaporation usually play only a minor role for ET, a reduction in

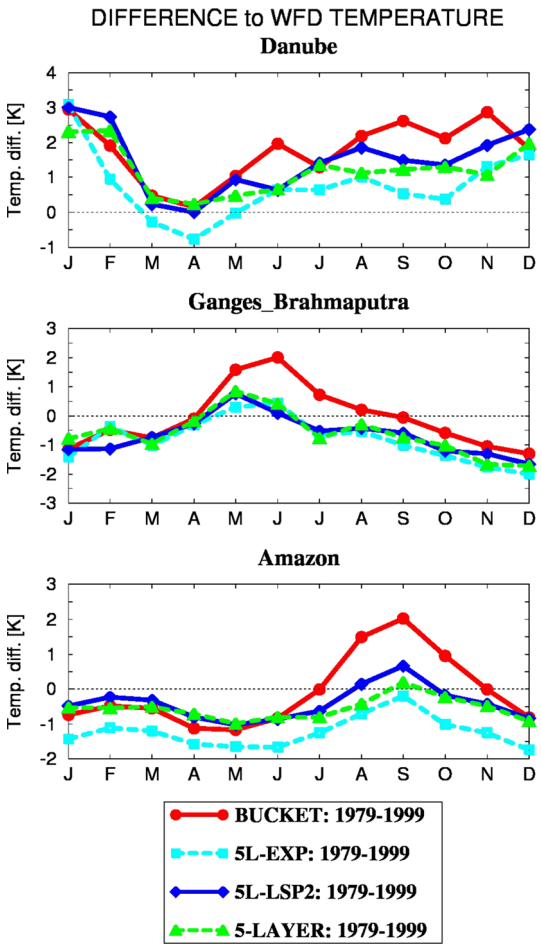

Fig. 11 Annual cycles of 2 m temperature differences to WFD data over selected catchments

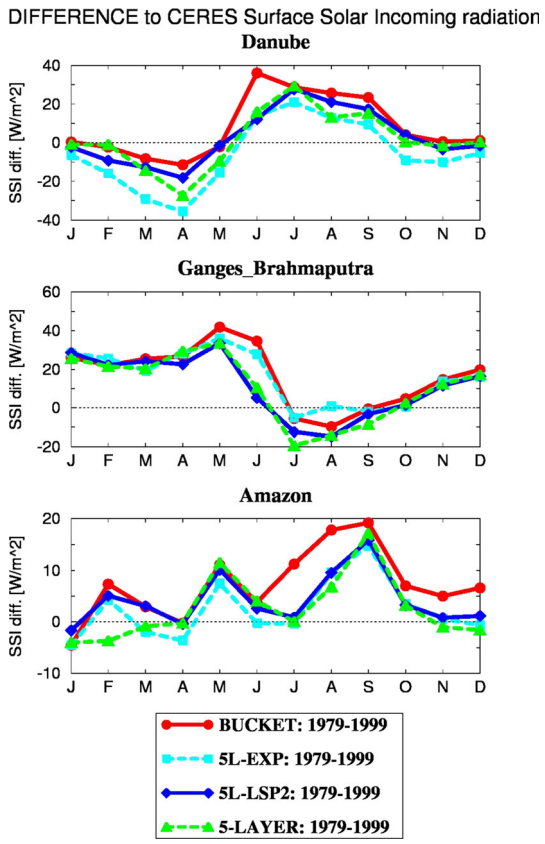

Fig. 12 Annual cycles of differences in surface solar incoming radiation (SSI) to CERES data (March 2000–February 2010) over selected catchments

bare soil evaporation often translates directly into an increase in transpiration (and vice versa). This is exemplarily shown for the Nile and Congo catchments in Fig. 16. Thus, a potential increase in soil moisture memory by reduced bare soil evaporation can easily be compensated by a decrease in memory due to increased transpiration. Consequently, the integrated effect on memory depends on the area and on the fact which of the evaporating processes is more efficient.

Using the new water holding capacities W_{cap} in 5-LAYER leads to general increases in soil moisture memory (Fig. 15c—left panel) where W_{cap} is decreasing (Fig. 2) and vice versa. As the soil depth z_s is not changing, a decrease in W_{cap} and, hence, z_r leads to an increase in the water storage below the root zone z_r. This means that more water is included in the slowly changing buffer that is only changed by vertical water transport within the soil according to Eq. (3), and less water in the faster changing root zone where soil moisture storage is affected by transpiration. Consequently, an increase of this buffer in soil moisture due to a decrease in W_{cap} generally leads to an enhanced soil moisture memory. This effect is very pronounced over the Euphrates catchment and can also be seen over the catchments of Mississippi, Nile and Euphrates (Fig. 14). However, this effect of a larger (smaller) buffer can be counteracted and partially compensated by enhanced (decreased) water fluxes between the buffer and the root zone due to the reduction (increase) of W_{cap}. These fluxes lead to higher (lower) variability of the buffer and, thus, tend to decrease (increase) the associated memory. This can be seen in the Parana (Congo) catchment (Fig. 14), where despite the buffer decrease (increase) a soil moisture memory increase (decrease) is seen for 5-LAYER compared to 5L-LSP2. For the Congo catchment, a reduced relative root zone soil moisture W_S/W_{cap} in 5-LAYER (not shown) also contributes to decreased water fluxes and lower buffer variability.

Note that for the Murray river, the buffer increases only slightly in 5-LAYER compared to 5L-LSP2. Here, some more precipitation is simulated in the second half of the year that leads to an increase in relative root zone soil

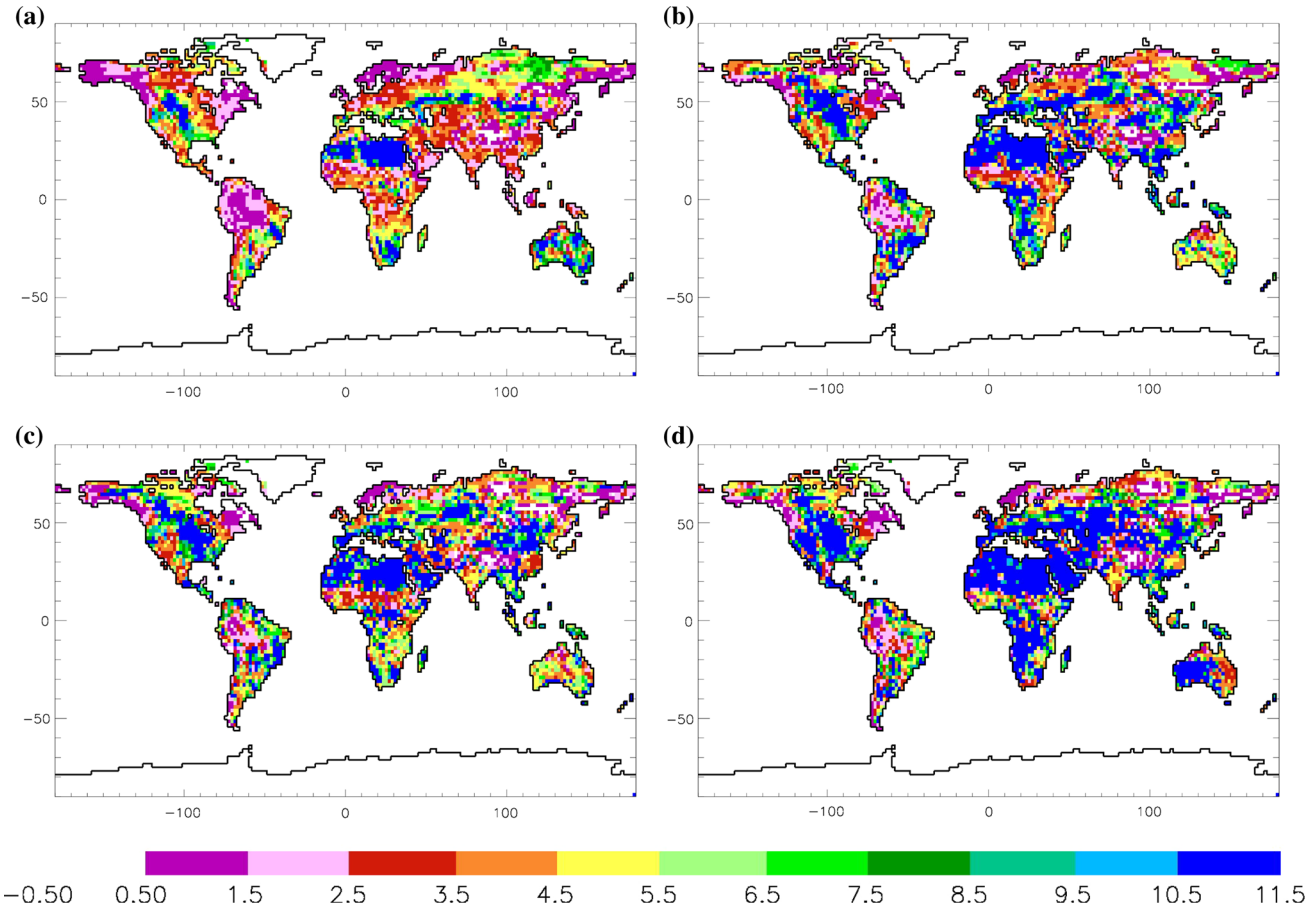

Fig. 13 Memory length in months with WS_{ges} autocorrelation continuously greater than 0.3. Correlation was calculated from monthly WS_{ges} anomalies for **a** BUCKET, **b** 5L-EXP, **c** 5L-LSP2, and **d** 5-LAYER

moisture from June to October (not shown). As even in this wet season, the catchment is relatively dry (with relative root zone soil moisture below 50 %), the wetter root zone causes an increase in vertical moisture fluxes and a subsequent larger soil moisture variability that in turn lead to a decrease in memory.

5 Summary and conclusions

In the present study, a new five layer soil hydrology scheme has been introduced to JSBACH, the land surface scheme of MPI-ESM. Four different setups of soil hydrology in JSBACH have been used to consider soil moisture memory at the global scale and to analyse how different characteristics of soil hydrology and the associated fluxes influence soil moisture memory. For this purpose, four setups were applied within ECHAM6/JSBACH simulations forced by AMIP2 SST and sea ice.

First, results from the new 5-layer scheme were compared to those obtained with the currently operational bucket scheme and to observations. The simulated mean climate and large-scale land surface water fluxes (precipitation, evapotranspiration, runoff) are largely kept between the different versions, showing slightly smaller biases in some variables and regions, and somewhat larger in others. Even though the general biases of the 2 m temperature and surface water fluxes don't change too much, the 5-layer scheme leads to more realistic representation of soil hydrological processes. This is especially the case for the evaporation over bare soil areas, which is prominent in arid and semi-arid regions. Here, with the 5-layer scheme, bare soil evaporation may now occur directly after rain events, which is hardly possible using the bucket scheme formulation. Also the buffering of soil moisture below the root zone seems to lead to an improved behaviour. This is at least the case over the Amazon catchment, where the 5-layer scheme yields an improved simulation of summer time 2 m temperatures due to the moisture supply from the buffer below the root zone. Consequently, for many catchments the root zone becomes drier in wet seasons, partially due to the improved and increased bare soil evaporation, and wetter in the dry season due to water supply from the water storage below root zone upward transport.

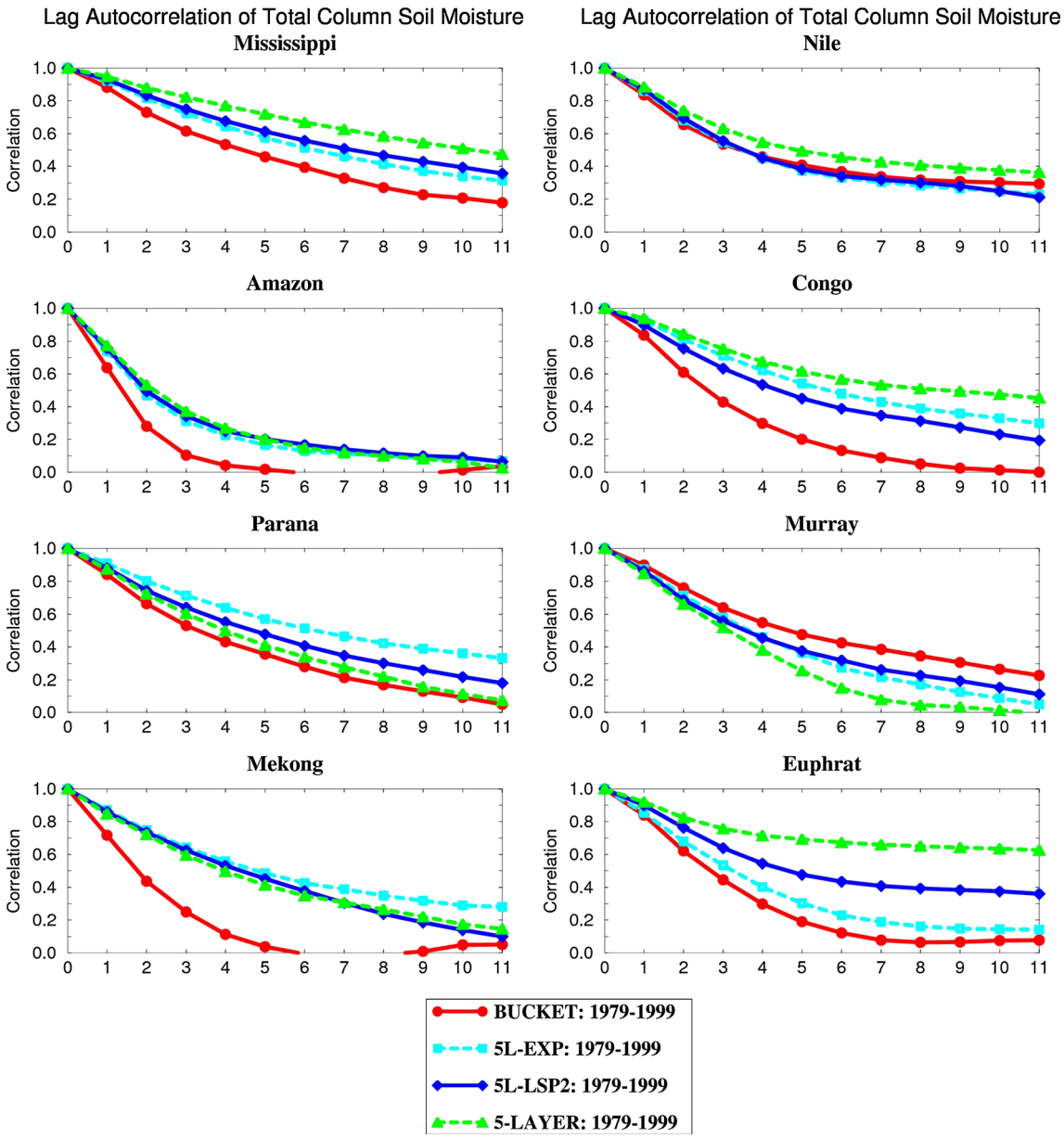

Fig. 14 Autocorrelation of total column soil moisture WS_{ges} as a function of the monthly lag over selected catchments

Soil moisture memory effects with time scales of one season or more are simulated over many parts of the globe, especially over the US, southern South America and Africa, Sahel, South and Central Europe, Australia, Caucasus and West Siberia, Southern China and Indochina. Here, memory diagnostics may be blurred in essentially dry (e.g. Sahara, Asian deserts, Australia) areas or regions where the soil is simulated to be almost continuously wet (Northern Siberia). The 5-layer scheme, due the water buffer below the root zone, increases soil moisture memory over large parts of northern and eastern US, northern and middle South America, Europe, South East Asia and Central Africa. It decreases memory, mainly due to the improved and enhanced bare soil evaporation in less vegetated areas, over eastern US, southern South America, Sahel and South Africa, Australia and Northern Siberia. In some areas, both effects on the memory seem to partially compensate each other, even though the increasing impact of the water buffer below the root zone often tends to be stronger. Generally, a reduction in the two evapotranspiration fluxes from the soil, bare soil evaporation and transpiration, increases the soil moisture memory. However, there is usually a strong interlink of both components by the atmospheric near-surface moisture demand so that increases in bare soil evaporation lead to decreases in transpiration and vice versa in areas where vegetation and

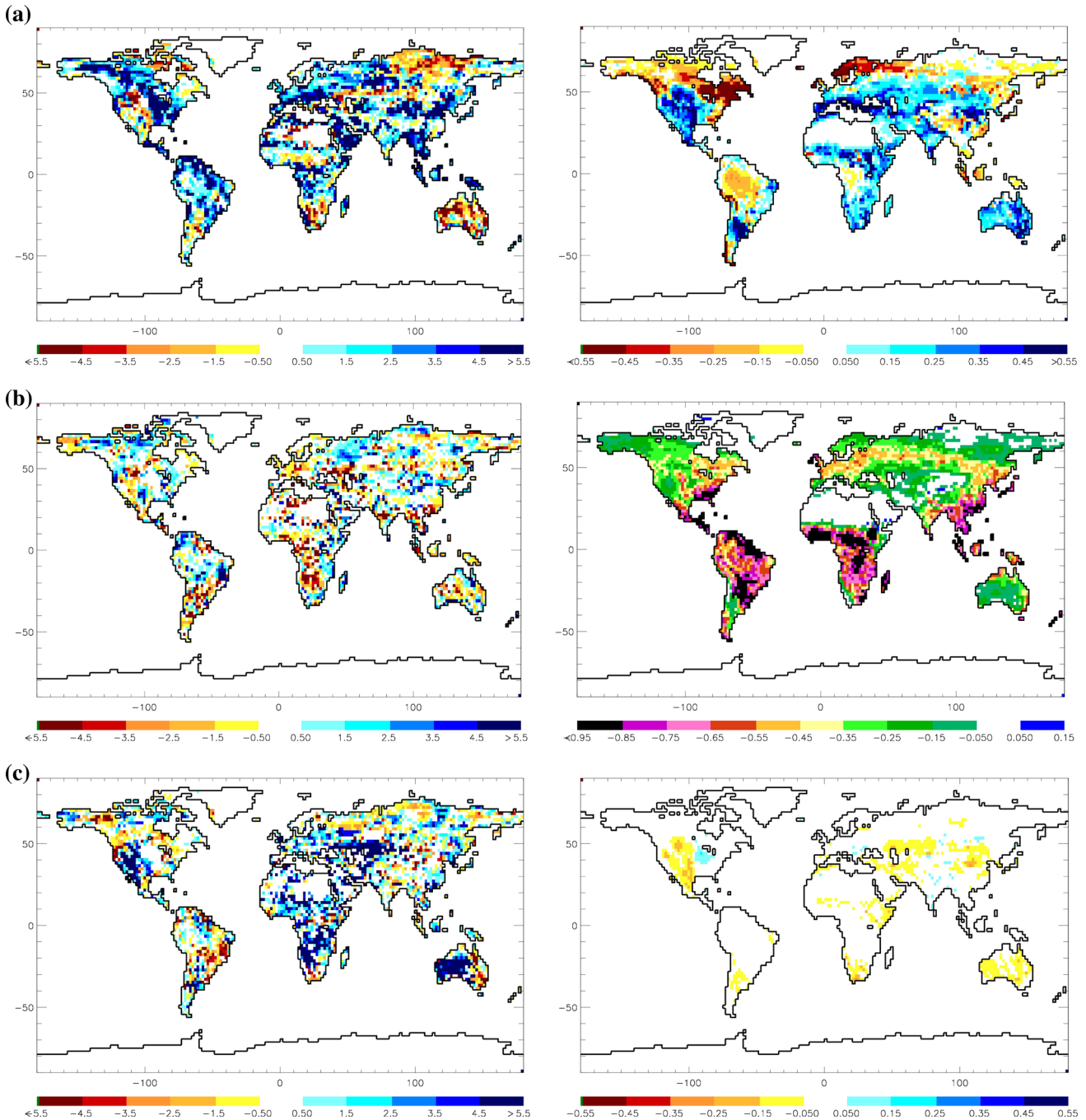

Fig. 15 Change in memory length in months with WS_{ges} autocorrelation continuously >0.3 (*left column*) and in bare soil evaporation (mm/day; *right column*) for **a** 5L-LSP2 minus BUCKET, **b** 5L-LSP2 minus 5L-EXP, and **c** 5-LAYER minus 5L-LSP2

bare soil coexist. Thus, the combined effect of changes in these fluxes on soil moisture memory strongly depends on the region and on which of both processes is more efficiently in varying the total column soil moisture.

If the total soil moisture storage is kept, reducing root zone soil moisture storage generally leads to an increase in soil moisture memory due to the enhanced soil water buffer storage below the root zone. This is in line with results of Asharaf and Ahrens (2013) who applied a regional climate model over the Indian monsoon region and found that simulated memory lengths increase with soil depth. Also here, it can be postulated that an increased soil depth usually is accompanied by an increased soil water buffer. The general effect of changed moisture storage can be regionally modulated by changes in water fluxes such as precipitation and transpiration.

The introduction of a layered soil hydrology that has the same vertical layer structure as used for soil temperatures is a

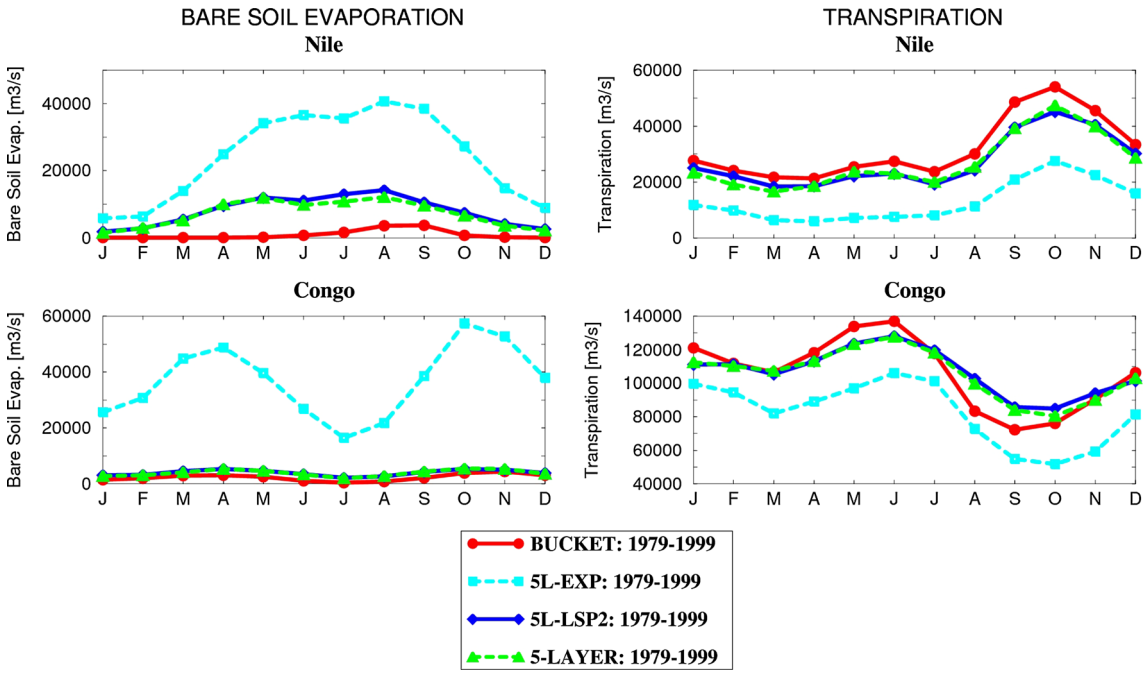

Fig. 16 Bare soil evaporation (*left panel*) and transpiration (*right panel*) averaged over the Nile and Congo catchments

necessary first step towards permafrost modelling and the associated simulation of melting and freezing of soil water. For the JSBACH model, the latter has been implemented recently into JSBACH by Ekici et al. (2013) whose results show a generally realistic behaviour of JSBACH with regard to cold region land surface processes. Within the German project MiKlip, the 5-LAYER version of JSBACH will be used to investigate soil moisture memory effects in models and observations with respect to seasonal and decadal forecasts.

Acknowledgments The present work was supported by funding for Stefan Hagemann from the European Commission's 7th Framework Programme, under Grant Agreement number 282672, within the EMBRACE project. Tobias Stacke acknowledges funding from the Federal Ministry of Education and Research in Germany (BMBF) through the research programme MiKlip (FKZ: 01LP1108A). Moreover, we would like to thank Veronika Gayler, Thomas Raddatz, Christian Reick, Reiner Schnur and Stiig Wilkenskjeld from MPI-M for helpful advice during the technical implementation of the 5-layer scheme into the JSBACH model.

References

Asharaf S, Ahrens B (2013) Soil-moisture memory in the regional climate model COSMO-CLM during the Indian summer monsoon season. J Geophys Res 118:6144–6151. doi:10.1002/jgrd.50429

Beringer J, Lynch AH, Chapin FS II, Mack M, Bonan GB (2001) The representation of Arctic soils in the land surface model: the importance of mosses. J Clim 14:3324–3335

Brovkin V, Raddatz T, Reick CH, Claussen M, Gayler V (2009) Global biogeophysical interactions between forest and climate. Geophys Res Lett 36(L07):405. doi:10.1029/2009GL037543

Caldwell MM, Dawson TE, Richards JH (1998) Hydraulic lift: consequences of water efflux from the roots of plants. Oecologia 113:151–161

Clapp RB, Hornberger GM (1978) Empirical equations for some soil hydraulic properties. Water Resourc Res 14:601–604

Dee DP, Uppala SM, Simmons AJ, Berrisford P, Poli P, Kobayashi S, Andrae U, Balmaseda MA, Balsamo G, Bauer P, Bechtold P, Beljaars ACM, van de Berg L, Bidlot J, Bormann N, Delsol C, Dragani R, Fuentes M, Geer AJ, Haimberger L, Healy SB, Hersbach H, Hólm EV, Isaksen L, Kållberg P, Köhler M, Matricardi M, McNally AP, Monge-Sanz BM, Morcrette J-J, Park B-K, Peubey C, de Rosnay P, Tavolato C, Thépaut J-N, Vitart F (2011) The era-interim reanalysis: configuration and performance of the data assimilation system. Q J R Meteorol Soc 137:553–597. doi:10.1002/qj.828,2011

Delworth TL, Manabe S (1988) The influence of potential evaporation on the variabilities of simulated soil wetness and climate. J Clim 1:523–547

Dirmeyer P, Koster R, Guo ZAD (2006) Do global models properly represent the feedback between land and atmosphere? J Hydrometeor 7:1177–1198

Disse M (1995) Modellierung der Verdunstung und der Grundwasserneubildung in ebenen Einzugsgebieten. *Mitteilungen des Inst. f.* Hydrologie u. Wasserwirtschaft d. Universität Karlsruhe 53:95–107

Dümenil Gates L, Hagemann S, Golz C (2000) Observed historical discharge data from major rivers for climate model validation. Max Planck Institute for Meteorology Rep 307 [available from MPI for Meteorology, Bundesstr. 53, 20146 Hamburg, Germany]

Dümenil L, Todini E (1992) A rainfall-runoff scheme for use in the Hamburg climate model. In: Kane JP (ed) Advances in theoretical hydrology—a tribute to James Dooge. Elsevier Science Publishers, Amsterdam, pp 129–157

Dunne KA, Wilmott CJ (1996) Global distribution of plant-extractable water capacity of soil. Int J Climatol 16:841–859

Ekici A, Beer C, Hagemann S, Hauck C (2013) Improved soil physics for simulating high latitude permafrost regions by the JSBACH terrestrial ecosystem model. Geosci Model Dev Discuss 6:2655–2698. doi:10.5194/gmdd-6-2655-2013

FAO/UNESCO (1971–1981) Soil map of the world, vols 1–10, UNESCO, Paris

Hagemann S (2002) An improved land surface parameter dataset for global and regional climate models. Max Planck Institute for Meteorology Rep 336, Max Planck Institute for Meteorology, Hamburg, Germany [Report available electronically from: http://www.mpimet.mpg.de/en/wissenschaft/publikationen.html]

Hagemann S, Dümenil L (1998) A parameterization of the lateral waterflow for the global scale. Clim Dyn 14:17–31

Hagemann S, Loew A, Andersson A (2013) Combined evaluation of MPI-ESM land surface water and energy fluxes. J Adv Model Earth Syst 5. doi:10.1029/2012MS000173

Hirschi M, Seneviratne SI, Alexandrov V, Boberg F, Boroneant C, Christensen OB, Formayer H, Orlowsky B, Stepanek P (2011) Observational evidence for soil-moisture impact on hot extremes in southeastern Europe. Nature Geosci 4:17–21. doi:10.1038/ngeo1032

Jackson RB, Sperry JS, Dawson TE (2000) Root water uptake and transport: using physiological processes in global predictions. Trend Plant Sci 5:482–488

Jiménez C, Prigent C, Mueller B, Seneviratne SI, McCabe M, Wood E, Rossow W, Balsamo G, Betts A, Dirmeyer P, Fisher J, Jung M, Kanamitsu M, Reichle R, Reichstein M, Rodell M, Sheffield J, Tu K, Wang K (2011) Global inter-comparison of 12 land surface heat flux estimates. J Geophys Res. doi:10.1029/2010JD014545

Kato S, Loeb NG, Rose FG, Doelling DR, Rutan DA, Caldwell TE, Yu L, Weller RA (2013) Surface irradiances consistent with ceres-derived top-of-atmosphere shortwave and longwave irradiances. J Clim 26:2719–2740. doi:10.1175/JCLI-D-12-00436.1

Kleidon A (2004) Global datasets and rooting zone depth inferred from inverse methods. J Climate 17:2714–2722

Koster RD, Suarez MJ (2001) Soil moisture memory in climate models. J Hydrometeor 2:558–570

Koster RD, Dirmeyer PA, Guo Z, Bonan G, Chan E, Cox P, Gordon CT, Kanae S, Kowalczyk E, Lawrence D, Liu P, Lu CH, Malyshev S, McAvaney B, Mitchell K, Mocko D, Oki T, Oleson K, Pitman A, Sud YC, Taylor CM, Verseghy D, Vasic R, Xue Y, Yamada T (2004a) Regions of strong coupling between soil moisture and precipitation. Science 305(5687):1138–1140

Koster RD, Suarez MJ, Liu P, Jambor U, Berg A, Kistler M, Reichle R, Rodell M, Famiglietti J (2004b) Realistic initialization of land surface states: impacts on subseasonal forecast skill. J Hydrometeor 5:1049–1063

Koster RD, Mahanama S, Yamada TJ, Balsamo G, Boisserie M, Dirmeyer P, Doblas-Reyes F, Gordon CT, Guo Z, Jeong J-H, Lawrence DM, Lee W-S, Li Z, Luo L, Malyshev S, Merryfield W, Seneviratne SI, Stanelle T, van den Hurk B, Vitart F, Wood EF (2010) The contribution of land initialization to subseasonal forecast skill: first results from the GLACE-2 Project. Geophys Res Lett 37:L02402. doi:10.1029/2009GL041677

Letts MG, Roulet NT, Corner NT, Skapura MR, Verseghy DL (2000) Parametrization of peatland hydraulic properties for the Canadian land surface scheme. Atmos Ocean 38(1):141–160

Liu YY, Parinussa RM, Dorigo W, De Jeu R, Wagner W, van Dijk IJM, McCabe MF, Evans JP (2011) Developing an improved soil moisture dataset by blending passive and active microwave satellite-based retrievals. Hydrol Earth Syst Sci 15:425–436. doi:10.5194/hess-15-425-2011

Loew A, Stacke T, Dorigo W, de Jeu R, Hagemann S (2013) Potential and limitations of multidecadal satellite soil moisture observations for climate model evaluation studies. Hydrol Earth Syst Sci 17:3523–3542. doi:10.5194/hess-17-3523-2013

Lorenz R, Jaeger EB, Seneviratne SI (2010) Persistence of heat waves and its link to soil moisture memory. Geophys Res Lett 37:L09703. doi:10.1029/2010GL042764

Mitchell KE, Lohmann D, Houser PR, Wood EF, Schaake JC, Robock A, Cosgrove BA, Sheffield J, Duan Q, Luo L, Higgins RW, Pinker RT, Tarpley JD, Lettenmaier DP, Marshall CH, Entin JK, Pan M, Shi W, Koren V, Meng J, Ramsay BH, Bailey AA (2004) The multi-institution North American land data assimilation system (NLDAS): utilizing multiple GCIP products and partners in a continental distributed hydrological modeling system. J Geophys Res 109:D07S90. doi:10.1029/2003JD003823

Mueller B, Seneviratne SI, Jimenez C, Corti T, Hirschi M, Balsamo G, Ciais P, Dirmeyer P, Fisher JB, Guo Z, Jung M, Maignan F, McCabe MF, Reichle R, Reichstein M, Rodell M, Sheffield J, Teuling AJ, Wang K, Wood EF, Zhang Y (2011) Evaluation of global observations-based evapotranspiration datasets and IPCC AR4 simulations. Geophys Res Lett 38. doi:10.1029/2010GL046230

O'Geen AT (2012) Soil water dynamics. Nature Educ Knowl 3(6):12

Patterson KA (1990) Global distributions of total and total-avaiable soil water-holding capacities. University of Delaware, Delaware

Raddatz TJ, Reick C, Knorr W, Kattge J, Roeckner E, Schnur R, Schnitzler K-G, Wetzel P, Jungclaus JH (2007) Will the tropical land biosphere dominate the climate-carbon cycle feedback during the twenty-first century? Clim Dyn. doi:10.1007/s00382-007-0247-8

Richards LA (1931) Capillary conduction of liquids through porous mediums. Physics 1(5):318–333. doi:10.1063/1.1745010

Richtmyer RD, Morton KW (1967) Difference methods for initial-value problems. Wiley-Interscience, New York

Rodell M, Houser PR, Jambor U, Gottschalck J, Mitchell K, Meng C-J, Arsenault K, Cosgrove B, Radakovich J, Bosilovich M, Entin JK, Walker JP, Lohmann D, Toll D (2004) The global land data assimilation system. Bull Am Meteorol Soc 85(3):381394

Roeckner E, Arpe K, Bengtsson L, Christoph M, Claussen M, Dümenil L, Esch M, Giorgetta M, Schlese U, Schulzweida U (1996) The atmospheric general circulation model ECHAM-4: model description and simulation of the present day climate. Max Planck Institute for Meteorology Rep 218. Available from MPI for Meteorology, Bundesstr. 53, 20146 Hamburg, Germany

Roesch A, Wild M, Gilgen H, Ohmura A (2001) A new snow cover fraction parameterization for the ECHAM4 GCM. Clim Dyn 17:933–946

Rowntree PR (1991) Atmospheric parameterization schemes for evaporation over land: basic concepts and climate modelling aspects, In: Schmugge TJ, Andre J (eds) Land surface evaporation—measurement and parameterization. Springer, Berlin, pp 5–29

Schlosser CA, Milly PCD (2002) A model-based investigation of soil moisture predictability and associated climate predictability. J Hydrometeor 3:483–501

Sellers PY, Mintz Y, Sud YC, Dalcher A (1986) A simple biosphere model (Sib) for use within general circulation models. J Atm Sci 43:505–531

Seneviratne SI, Stöckli R (2008) The role of land-atmosphere interactions for climate variability in Europe. In: Brönnimann et al (eds) Climate variability and extremes during the past 100 years. Adv Global Change Res 33. Springer, Berlin (Book chapter)

Seneviratne SI, Koster RD, Guo Z, Dirmeyer PA, Kowalczyk E, Lawrence D, Liu P, Lu C-H, Mocko D, Oleson KW, Verseghy D (2006a) Soil moisture memory in AGCM simulations: analysis

of global land–atmosphere coupling experiment (GLACE) data. J Hydrometeor 7:1090–1112

Seneviratne SI, Lüthi D, Litschi M, Schär C (2006b) Land–atmosphere coupling and climate change in Europe. Nature 443:205–209

Seneviratne SI, Corti T, Davin E, Hirschi M, Jaeger EB, Lehner I, Orlowsky B, Teuling AJ (2010) Investigating soil moisture–climate interactions in a changing climate: a review. Earth-Sci Rev 99:125–161. doi:10.1016/j.earscirev.2010.02.004

Stevens B, Giorgetta M, Esch M, Mauritsen T, Crueger T, Rast S, Salzmann M, Schmidt H, Bader J, Block K, Brokopf R, Fast I, Kinne S, Kornblueh L, Lohmann U, Pincus R, Reichler T, Roeckner E (2013) The atmospheric component of the MPI-M earth system model: ECHAM6. J Adv Model Earth Syst 5:146–172. doi:10.1002/jame.20015

Taylor CM, Ellis RJ (2006) Satellite detection of soil moisture impacts on convection at the mesoscale. Geophys Res Lett 33:L03404. doi:10.1029/2005GL025252

Taylor KE, Williamson D, Zwiers F (2000) The sea surface temperature and sea-ice concentration boundary conditions for AMIP II simulations. PCMDI Report, 60, program for climate model diagnosis and intercomparison. Lawrence Livermore National Laboratory, Livermore, California, 25 pp

Van Genuchten MT (1980) A closed-form equation for predicting the hydraulic conductivity of unsaturated soils. Soil Sci Soc Am J 44:892–898

Warrilow DA, Sangster AB, Slingo A (1986) Modelling of land surface processes and their influence on European climate. UK Met Office Tech Note DCTN 38, 92 pp

Weedon GP, Gomes S, Viterbo P, Shuttleworth WJ, Blyth E, Österle H, Adam JC, Bellouin N, Boucher O, Best M (2011) Creation of the WATCH forcing data and its use to assess global and regional reference crop evaporation over land during the twentieth century. J Hydrometeor 12:823–848. doi:10.1175/2011JHM1369.1

Williams RD, Ahuja LR (2003) Scaling and estimating the soil water characteristic using a one-parameter model. In: Pachepsky Y, Radcliffe DE, Selim HM (eds) Scaling methods in soil physics. CRC Press, Boca Raton, pp 35–48